Micromechanical Modeling of Interfacial Debonding in Silicon Dioxide/AA3003 Alloy Particle-Reinforced Metal Matrix Composites

[1]S. Sundara Rajan and A. Chennakesava Reddy[2]

[1]Scientist-F, Defence Research and Development Organisation, Hyderabad, India.
[2]Assistant Professor, Department of Mechanical Engineering, MJ College of Engineering and Technology, Hyderabad, India
dr_acreddy@yahoo.com

Abstract: *A diamond array unit cell/ellipsoidal SiO_2 nanoparticle RVE models were used to evaluate micromechanical behavior and interfacial debonding in AA3003/SiO_2 composites. The AA3003/SiO_2 particulate metal matrix composites were fabricated at different volume fractions of SiO_2. The chemical reaction was observed at the interface between AA3003 alloy and SiO_2 particles. The interfacial debonding was observed in all the composites.*

Keywords: AA3003*, silicon dioxide, ellipsoidal nanoparticle, RVE model, finite element analysis, debonding.*

1. INTRODUCTION

The technique to improve mechanical performance of materials by dispersing particles in a matrix has been applied to ceramic-matrix, metal-matrix and polymer-matrix composites, and these materials are called particulate-reinforced composites. In particulate-reinforced composites, a variety of damage modes such as fracture of particles, interfacial debonding between particles and matrix, and cracking in matrix adjacent to hard particles develop from an early stage of deformation under monotonic and cyclic loads. These damage modes strongly affect mechanical performances such as stress-strain relation, tensile strength and fracture toughness [1, 2]. A study was conducted on the silane interfacial effect on the fracture process of embedded single E-glass fiber [3]. The interfacial reinforcement reflects the progressed fracture rather than the instantaneous fracture. A variety of nanoparticles such as silicon nitride [4, 5], titanium oxide [6, 7], graphite [8], titanium carbide [9, 10], boron nitride [11], zirconium oxide [12], titanium nitride [13], titanium boride [14], zirconium carbide [15], silicon oxide [16], magnesium oxide [17] at 10%, 20% and 30% volume fractions were studied and the results computed from a unit cell with uniformly distributed particles were compared. The influence of progressive damage on stress-strain relation of particulate-reinforced composites was studied with two schemes. Finite element analysis for a unit cell containing one particle in a matrix was widely applied to fracture or debonding of particles [18]. The unit cell analysis has an advantage to provide details of damage process in one particle [4-17].

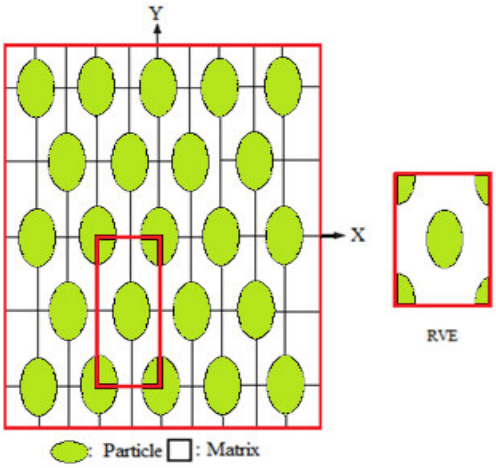

Figure 1: A diamond RVE containing an ellipsoidal nanoparticle.

Silicon dioxide is a chemical compound that is an oxide of silicon with the chemical formula SiO_2. Silicon dioxide is mostly obtained by mining and purification of quartz. In its capacity as a refractory, it is useful in fiber form as a high-temperature thermal protection fabric. SiO_2 has a number of distinct crystalline forms (polymorphs) in addition to amorphous forms. With the exception of stishovite and fibrous silica, all of the crystalline forms involve tetrahedral SiO_4 units linked together by shared vertices in different arrangements. Silicon–oxygen bond lengths vary between the different crystal forms, for example in

α-quartz the bond length is 161 pm, whereas in α-tridymite it is in the range 154–171 pm. The Si-O-Si angle also varies between a low value of 140° in α-tridymite, up to 180° in β-tridymite. In α-quartz the Si-O-Si angle is 144°. The reason to take up this work was to examine interfacial debonding and fracture of silicon oxide nanoparticles in the AA3003 alloy/SiO_2 nanoparticle composites using RVE model through finite element analysis. Shape of the reinforced particle considered in this work is a ellipsoidal. The periodic particle distribution was a diamond array as shown in figure 1.

2. THEORETICAL BACKGROUND

The strains along x- and y-directions can be determined as using the following equations:

$$\varepsilon_y = -\left(\frac{v_{xy}}{E_x} + \frac{1}{E_z}\right)P = \frac{\Delta y}{a} \quad (1)$$

$$\varepsilon_x = \left(\frac{1}{E_x} - \frac{1}{E_z}\right)P = \frac{\Delta x}{a} \quad (2)$$

The effective elastic moduli and Poisson's ratio in the transverse direction (xy-plane) as follows:

$$E_x = \frac{1}{\frac{\Delta x}{Pa} + \frac{1}{E_z}} \text{ and } E_y = \frac{1}{\frac{\Delta y}{Pa} + \frac{1}{E_z}} \quad (3)$$

$$v_{xy} = \left(\frac{\Delta y}{Pa} + \frac{1}{E_z}\right)/\left(\frac{\Delta x}{Pa} + \frac{1}{E_z}\right) \quad (4)$$

Once the change in lengths along x- and y- direction (Δx and Δy) are determined for the square RVE from the FEA, E_y and E_x and v_{xy} can be determined from Eqs. (3) and (4), correspondingly. Considering adhesion, formation of precipitates, particle size, agglomeration, voids/porosity, obstacles to the dislocation, and the interfacial reaction of the particle/matrix, the formula for the strength of composite is stated below:

$$\sigma_c = \left[\sigma_m\left\{\frac{1-(v_p+v_v)^{2/3}}{1-1.5(v_p+v_v)}\right\}\right]e^{m_p(v_p+v_v)} + kd_p^{-1/2} \quad (5)$$

$$k = E_m m_m / E_p m_p$$

where, v_v and v_p are the volume fractions of voids/porosity and nanoparticles in the composite respectively, m_p and m_m are the possion's ratios of the nanoparticles and matrix respectively, d_p is the mean nanoparticle size (diameter) and E_m and E_p is elastic moduli of the matrix and the particle respectively. Elastic modulus (Young's modulus) is a measure of the stiffness of a material and is a quantity used to characterize materials. Elastic modulus is the same in all orientations for isotropic materials. Anisotropy can be seen in many composites.

The upper-bound equation is given by

$$\frac{E_c}{E_m} = \left(\frac{1-v_v^{2/3}}{1-v_v^{2/3}+v_v}\right) + \frac{1+(\delta-1)v_p^{2/3}}{1+(\delta-1)(v_p^{2/3}-v_p)} \quad (6)$$

The lower-bound equation is given by

$$\frac{E_c}{E_m} = 1 + \frac{v_p - v_p}{\delta/(\delta-1)-(v_p+v_v)^{1/3}} \quad (7)$$

where, $\delta = E_p/E_m$.

The transverse modulus is given by

$$E_t = \frac{E_m E_p}{E_m + E_p(1-v_p^{2/3})/v_p^{2/3}} + E_m\left(1 - v_p^{2/3} - v_v^{2/3}\right) \quad (8)$$

3. MATERIALS METHODS

The matrix material was AA3003 aluminum alloy. The reinforcement material was ellipsoidal silicon oxide nanoparticles of average size 100nm. The mechanical properties of materials used in the present work are given in table 1.

Table 1: Mechanical properties of AA3003 matrix andSiO_2 nanoparticles

Property	AA3003	SiO_2
Density, g/cc	2.73	2.20
Elastic modulus, GPa	68.90	73.10
Ultimate tensile strength, MPa	155	-
Poisson's ratio	0.33	0.17

AA3003 alloy/SiO_2 composites were manufactured by the stir casting process and low pressure casting technique with argon gas at 3.0 bar. The composite samples were give solution treatment and cold rolled to the predefined size of tensile specimens.

The heat-treated samples were machined to get flat-rectangular specimens (figure 2) for the tensile tests. The tensile specimens were placed in the grips of a Universal Test Machine (UTM) at a specified grip separation and pulled until failure. The test speed was 2 mm/min (as for ASTM D3039). A strain gauge was used to determine elongation.

In this research, a cubical representative volume element (RVE) was implemented to analyze the tensile behavior AA3003/ SiO_2 nanoparticle composites at three (10%, 20% and 30%) volume fractions of SiO_2. The large strain PLANE183 element was used in the matrix in all the models. In order to model the adhesion between the matrix and the particle, a CONTACT 172 element was used.

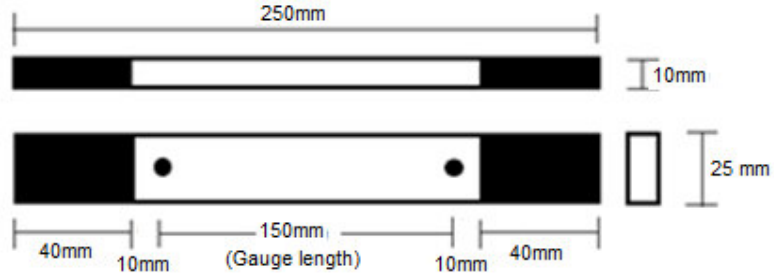

Figure 2: Shape and dimensions of tensile specimen

4. RESULTS AND DISCUSSION

The micromechanical behavior is discussed in terms of tensile elastic moduli, E_x, shear modulus, G_{xy} and major Poisson's ratio, v_{xy}. The fracture behavior is conversed in terms of interface debonding and particle fracture.

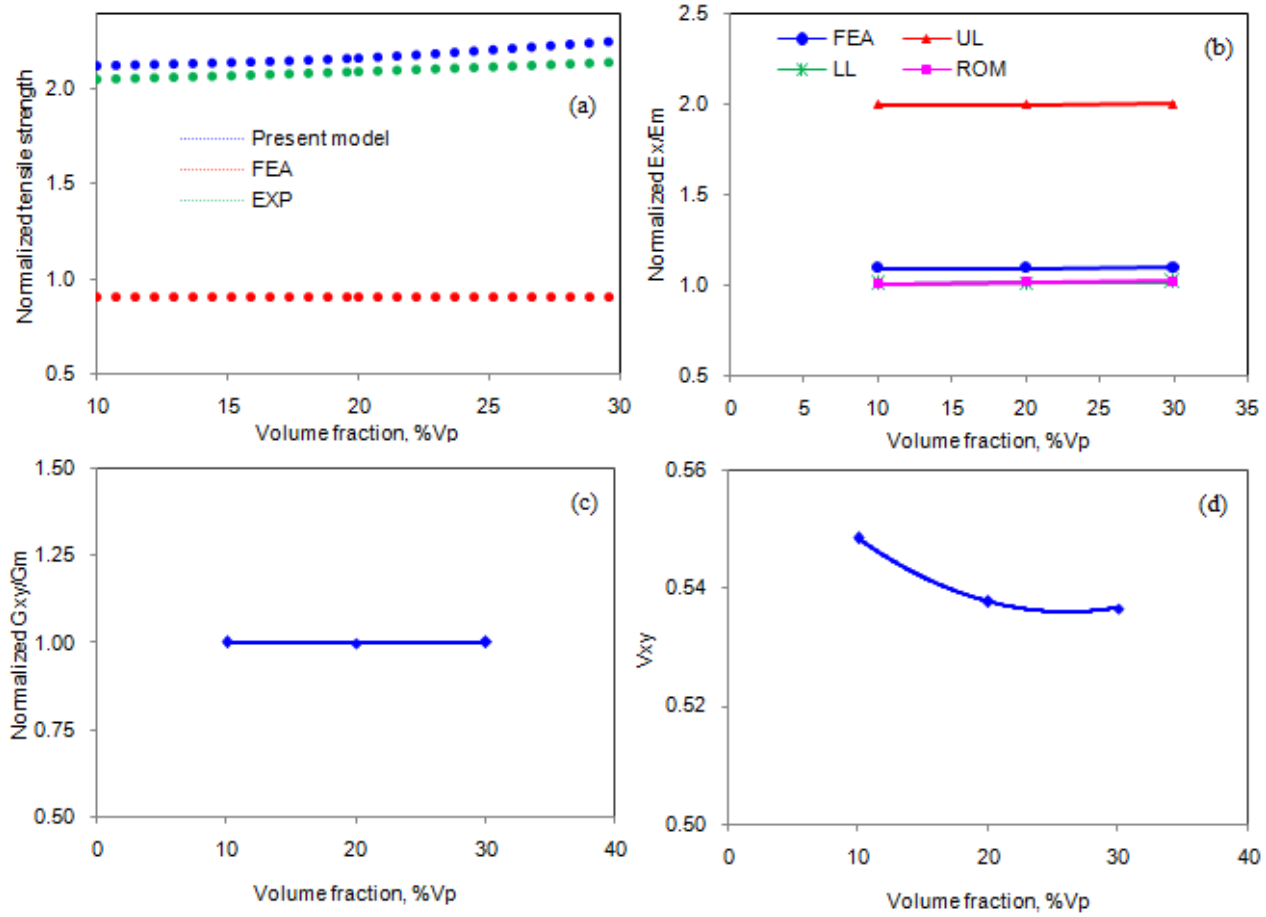

Figure 3: Effect of volume fraction on micromechanical behavior of AA3003/SiO_2 composites.

4.1 Micromechanical Behavior

Figure 3a depicts the normalized tensile strengths of the AA3003 alloy/SiO_2 composites obtained by FEA, present mathematical model, and experimental test. The tensile strength is normalized with ultimate tensile strength of AA3003 alloy matrix. The results obtained from present mathematical model and the experimental procedures are nearly same. The difference between the results obtained from experimental procedure and the FEA is very high. This is due to the ignorance of metallurgical phenomenon such as reaction between SiO_2 nanoparticles and AA3003 alloy matrix. The reduction of SiO_2 by Al was studied in Al/SiO_2/Si structures above 350 °C. It was found that Al displaces Si in the oxide, forming an Al–O compound with an Al:O concentration ratio between 1:1 and 1.3:1 [19]. The Al-Si system (figure 4) is a simple binary eutectic with limited solubility of aluminum in silicon and limited solubility of silicon in aluminum. The solubility of silicon in aluminum reaches a maximum 1.5 % at the eutectic temperature, and the solubility of silicon increases with temperature to 0.016% Si at 1190 °C. The eutectic reaction takes place at 577°C and at a silicon level of 12.6%. The formation of reactive compound as interface between Al-Si alloy and SiO_2 particle is shown in figure 5.

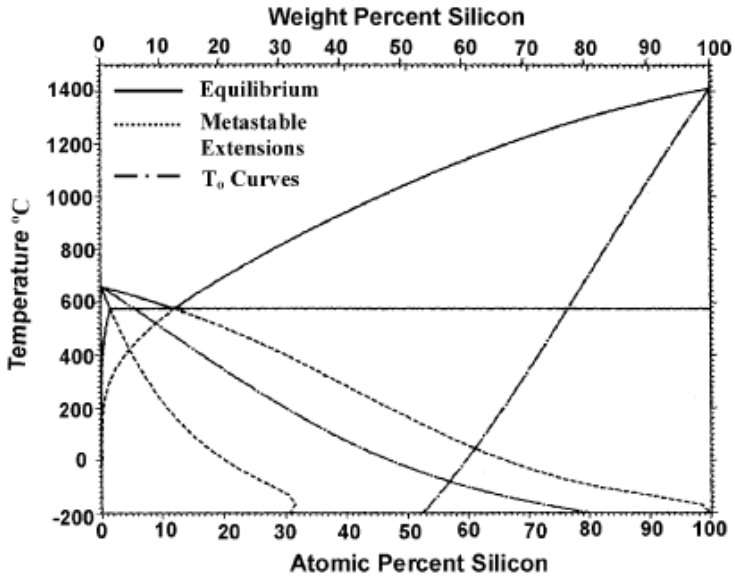

Figure 4: The equilibrium phases diagram for Al-Si system showing metastable extensions of liquidus and solidus lines.

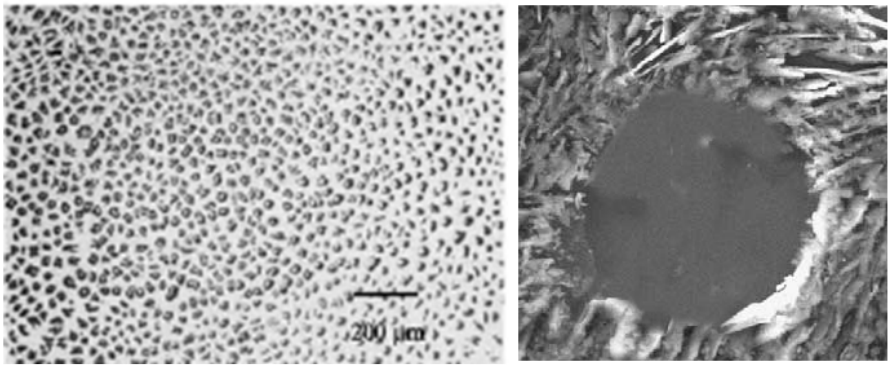

Figure 5: Al–Si alloy with interface around SiO_2 particle.

The normalized elastic modulus is shown in figure 3b. The elastic modulus is normalized with the elastic modulus of AA3003 alloy matrix. From the results obtained from the mathematical computation and test procedure, the stiffness of the composites is nearly constant with increase of volume fraction of SiO_2. This is because if very marginal difference in the elastic moduli of AA3003 alloy and SiO_2 particles.. The upper limit (UL) values computed by the present mathematical model are higher than those values obtained by the 'Role of Mixtures (ROM)'and FEA. This is because of consideration of voids in the present mathematical model. The shear strength of the composites is also unaffected with increase in the volume fraction of SiO_2 (figure 3c). The major Poisson's ratio decreases with increase of volume fraction of SiO_2 particles (figure 3d).

4.2 Fracture Analysis

If the particle deforms in an elastic manner (according to Hooke's law) then,

$$\tau = \frac{n}{2}\sigma_p \quad (9)$$

where σ_p is the particle stress. If particle fracture occurs when the stress in the particle reaches its ultimate tensile strength, $\sigma_{p,uts}$, then setting the boundary condition at

$$\sigma_p = \sigma_{p,\,uts} \quad (10)$$

The relationship between the strength of the particle and the interfacial shear stress is such that if

$$\sigma_{P,uts} < \frac{2\tau}{n} \quad (11)$$

Then the particle will fracture. From the figure 6b, it is observed that the SiO_2 nanoparticle was not fractured as the condition in Eq. (11) is not satisfied. For the interfacial debonding/yielding to occur, the interfacial shear stress reaches its shear strength:

$$\tau = \tau_{max} \quad (12)$$

For particle/matrix interfacial fracture can occur if the following condition is satisfied:

$$\tau_{max} < \frac{n\sigma_p}{2} \quad (13)$$

It is observed from figure 6a that the interfacial debonding occurs between SiO_2 nanoparticle and AA3003 alloy matrix as the condition in Eq.(13) is satisfied.

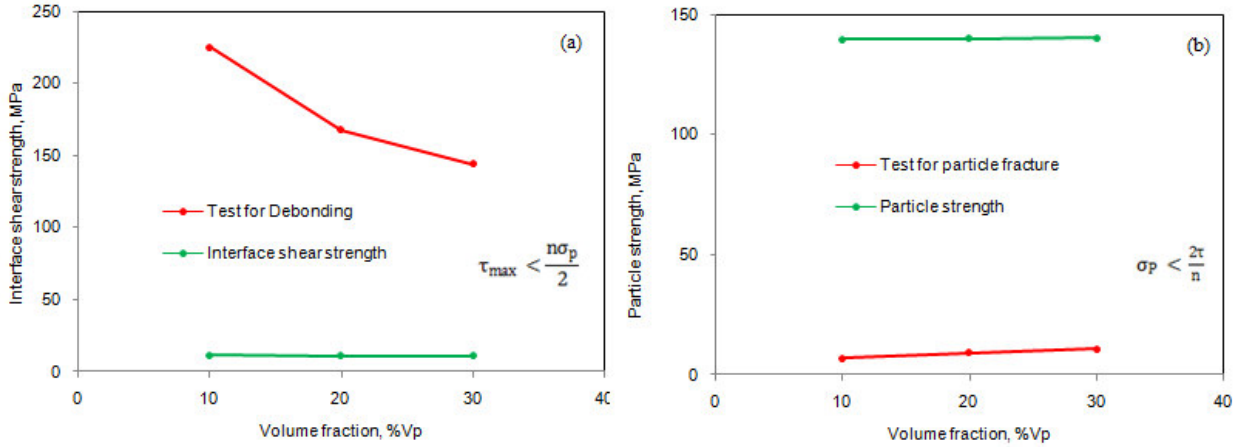

Figure 6: Criterion interfacial debonding (a) and for particle fracture (b).

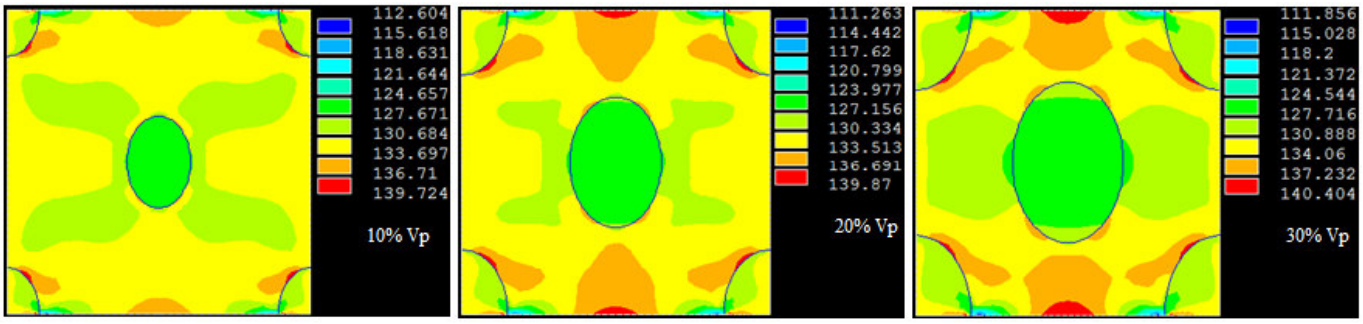

Figure 7: Images of tensile stress obtained from FEA.

As seen from 7 the tensile stress developed in the matrix are higher than those induced in the nanoparticle. The stress induced around the nanoparticle is higher than those induced in the SiO_2 particle. Hence, the interfacial debonding was occurred between the particle and the matrix.

5. CONCLUSION

The interfacial reaction is observed between AA3003 alloy matrix and SiO_2 reinforced particles. The experimental results are higher than those computed from FEA software owing to the ignorance of chemical reaction in the simulation. The interfacial debonding is resulted due to the tensile loading in AA3003 alloy/SiO2 composites.

REFERENCES

1. A. F. Whitehouse, T. W. Clyne,Cavity formation during tensile straining of particulate and short fibre metal matrix composites, Acta Metallurgica and Materialia, 41, 1993, pp.1701-1711.
2. S. F. Corbin, Wilkinson DS. Influence of matrix strength and damage accumulation on the mechanical response of a particulate metal matrix composite, Acta Metallurgica and Materialia, 42, 1994, pp.1329-1335.
3. B. Kotiveerachari, A. Chennakesava Reddy, Interfacial effect on the fracture mechanism in GFRP composites, CEMILAC Conference, Ministry of Defence, India, 20-21st August 1999.
4. A. Chennakesava Reddy, Assessment of Debonding and Particulate Fracture Occurrences in Circular Silicon Nitride Particulate/AA5050 Alloy Metal Matrix Composites , National Conference on Materials and Manufacturing Processes, Hyderabad, India, 27-28 February 1998, pp. 104-109.
5. A. Chennakesava Reddy, Evaluation of Debonding and Dislocation Occurrences in Rhombus Silicon Nitride Particulate/AA4015 Alloy Metal Matrix Composites, 1st National Conference on Modern Materials and Manufacturing , Pune, India, 19-20 December 1997, pp. 278-282.
6. S. Sundara Rajan, A. Chennakesava Reddy, Deformation Behavior of AA8090/ TiO_2 Nanoparticulate Reinforced Metal Matrix Composites with Debonding Interfaces, 2nd International Conference on Composite Materials and Characterization, Nagpur, India, 9-10 April 1999, pp. 245-248.
7. A. Chennakesava Reddy, Cohesive Zone Finite Element Analysis to Envisage Interface Debonding in AA7020/Titanium Oxide Nanoparticulate Metal Matrix Composites , 2nd International Conference on Composite Materials and Characterization, Nagpur, India, 9-10 April 1999, pp. 204-209.
8. A. Chennakesava Reddy, Micromechanical Modelling of Interfacial Debonding in AA1100/Graphite Nanoparticulate Reinforced Metal Matrix Composites, 2nd International Conference on Composite Materials and Characterization, Nagpur, India, 9-10 April 1999, pp. 249-253.
9. A. Chennakesava Reddy, Local Stress Differential for Particulate Fracture in AA2024/Titanium Carbide Nanoparticulate Metal Matrix Composites, National Conference on Materials and Manufacturing Processes, Hyderabad, India, 27-28 February 1998, pp. 127-131.
10. B. Kotiveera Chari, A. Chennakesava Reddy, Effect of Debonding on Overall Behavior of AA3003/Titanium Carbide Nanoparticulate Reinforced Metal Matrix Composites, 2nd International Conference on Composite Materials and Characterization, Nagpur, India, 9-10 April 1999, pp. 220-224.
11. H. B. Niranjan, A. Chennakesava Reddy, Effect of Particulate Debonding in AA5050/Boron Nitride Nanoparticulate Reinforced Metal Matrix Composites, 2nd International Conference on Composite Materials and Characterization, Nagpur, India, 9-10 April 1999, pp. 230-234.
12. P. M. Jebaraj, A. Chennakesava Reddy, Interface Debonding Prediction Technique for Tensile Loaded AA6061/Zirconium Oxide Nanoparticulate MMC, 2nd International Conference on Composite Materials and Characterization, Nagpur, India, 9-10 April 1999, pp. 235-239.
13. S. Sundara Rajan, A. Chennakesava Reddy, FEM Model for Volume Fraction Dependent Interface Debonding in TiN Nanoparticle Reinforced AA7020 Metal Matrix Composites, 2nd International Conference on Composite Materials and Characterization, Nagpur, India, 9-10 April 1999, pp. 240-244.
14. A. Chennakesava Reddy, Interfacial Debonding Analysis in Terms of Interfacial Tractions for Titanium Boride/AA3003 Alloy Metal Matrix Composites, 1st National Conference on Modern Materials and Manufacturing , Pune, India, 19-20 December 1997, pp. 124-127.
15. B. Kotiveera Chari, A. Chennakesava Reddy, Interfacial Debonding Analysis in Nanoparticulate Reinforced Metal Matrix Composites of AA8090/Zirconium Carbide, 2nd International Conference on Composite Materials and Characterization, Nagpur, India, 9-10 April 1999, pp. 210-214.
16. H. B. Niranjan, A. Chennakesava Reddy, Debonding Failure and Volume Fraction Effects in Nano-reinforced Composites of AA2024/Silicon Oxide, 2nd International Conference on Composite Materials and Characterization, Nagpur, India, 9-10 April 1999, pp. 215-219.
17. P. M. Jebaraj, A. Chennakesava Reddy, Analysis of Debonding along Interface of AA4015/Magnesium Oxide Nanoparticulate Reinforced Metal Matrix Composites, 2nd International Conference on Composite Materials and Characterization, Nagpur, India, 9-10 April 1999, pp. 225-229.
18. M. Finot, Y. L. Shen, A. Needleman, S. Suresh, Micromechanical modeling of reinforcement fracture in particle-reinforced metal-matrix composites, Metallurgical and Material Transaction, 25A, 1994, pp. 2403-2420.
19. F. Dadabhai, F. Gaspari, S. Zukotynski, C. Bland, Reduction of silicon dioxide by aluminum in metal–oxide–semiconductor structures, Journal of Applied Physics, 80, 1996, http://dx.doi.org/10.1063/1.363669.